Understanding the role α7 nicotinic receptors play in dopamine efflux in nucleus accumbens

Reinoud Maex *†, Vladimir Grinevich ‡§, Valentina Grinevich §, Evgeny Budygin §||, Merouane Bencherif ‡, Boris Gutkin †⊥

† Department of Cognitive Sciences, École Normale Supérieure, Paris, France
‡ Targacept Inc., Winston-Salem, NC, USA
§ Wake Forest School of Medicine, Winston-Salem, NC, USA
|| St. Petersburg State University, St. Petersburg, Russia
⊥National Research University Higher School of Economics, Center for Cognition and Decision Making, Moscow, Russia

Contents

Supplementary modeling results

Analysis of the drop in dopamine release, as produced in models based on the desensitization versus activation of α7 NNRs

We simulated the responses of two versions of the model to the same stimulation pattern: the partial α7 agonist TC-7020 and nicotine were systemically applied with a 30-s interval (upward arrows in Fig. S2 E). Note that the dopamine response of the model depended on two balances: that between receptor activation and desensitization, and that between excitation and inhibition of the dopamine neuron. As explained in the main text, the desensitization model represented the case where the α7 agonist desensitized NNRs located on the dopamine neuron itself or excitatory terminals afferent to it, with little or no influence from GABA neurons (see Fig. 2A). In the activation model α7 agonists reduced dopamine release by activating NNRs located on glutamatergic afferents to GABAergic interneurons in the VTA (Fig. 3A).

Figure S2 shows the time-course of the key model variables. Most importantly, both the desensitization model (left) and the activation model (right) generated the observed drop in dopamine release after TC-7020 administration, followed by a brisk rise after nicotine injection (Fig. S2 A). A distinctive feature, however, was that the activity of the GABA neurons slightly increased after TC-7020 injection in the activation model (red curve in right panel of Fig. S2 B), whereas it fell concomitantly with the drop in activity of the dopamine neurons in the desensitization model (panel B left). Indeed, in the desensitization model, with 80% of both α7s and α4β2s located on the dopamine neuron (or its afferents), the response of the GABA neuron was a scaled-down version of the dopamine neuron's response, and the GABA neuron decreased its spike rate after TC-7020 injection because of desensitization of the residual 20% of α7s that were located on its glutamatergic afferents. (Note that the baseline levels of activity of the dopamine and GABA neurons in Fig. S2 B are irrelevant for the present study. They can easily be reversed by introducing an additional free parameter, which we avoided for the sake of clarity.)

It is further clear from the fractions of open channels in panels Fig. S2 C that, in both models, the TC-7020 response was exclusively mediated by the α7 NNRs

(desensitization vs activation), whereas the nicotine response was dominated by activation (and subsequent desensitization) of the α4β2∗ channels.

For desensitization of the α7 NNRs to cause a noticeable drop in dopamine release, however, a background receptor activation by acetylcholine was needed (Fig. S2 C, left). In contrast, no cholinergic tone was needed to disclose the dopamine drop in the activation model (Fig. S2 C, right). Finally, the two models used different peak concentrations and time-courses for the applied TC-7020. The reason for using different peak concentrations is that these two models operate in different domains of the dose-response curve (see Fig. 5). In the activation model, the sustained presence of TC-7020 at a low concentration was needed to keep the NNRs activated, without desensitizing them all, during the whole interval of reduced dopamine release. In the desensitization model, in contrast, most of the NNRs completely desensitized and the drop in dopamine release would persist even after complete wash-out of the compound, owing to the slowness of resensitization as compared to activation. We used a faster pharmaco-kinetics for TC-7020 in the desensitization model to illustrate this latter phenomenon (compare Fig. S2 E, left vs right). The responses to slower (faster) kinetics are shown as gray traces. Note also that the reponse latencies (6-7 s in the experiments) were not modeled explicitly, but assumed to be generated by the systemic blood circulation, and by buffering in the pulmonary capillary bed (*1*).

Comparative model analysis

The effect of cholinergic tone

The critical effect of the level of the cholinergic tone is illustrated in greater detail in Figure S3. Clearly, a cholinergic tone was essential to the desensitization model (Fig. S3 A), but unnecessary, or even detrimental, in the activation model (Fig. S3 B).

In the desensitization model (Fig. S3 A), a weak or absent tone would reverse the observed effect of TC-7020 into an enhanced dopamine efflux (blue curve around 40 s), because of the default activation of α7 NNRs by partial agonists. In the presence of a higher cholinergic tone, however, TC-7020 did not only contribute less to receptor activation (because of saturation, and competition with acetylcholine), but it caused an even greater loss of acetylcholine-evoked current by desensitizing the

receptor. Stated otherwise, when TC-7020 desensitizes half of the α7 NNRs, it not only reduces its own effect by 50%, but also makes 50% of the receptors unavailable for the background physiological action of acetylcholine, and the latter effect is greater in absolute value the higher the tone. Much of this desensitization effect will go unnoticed in the absence of a cholinergic tone, whence our need of a higher tone in the desensitization model.

The activation model (Fig. S3 B), in contrast, showed an opposite dependency on cholinergic tone: a high tone would unmask desensitization of the α7 NNRs on the GABA neurons' afferents (red trace in inset to Fig S3 B). The resulting drop in activity of the GABA neurons disinhibited the dopamine neurons, so that, after a transient drop, dopamine efflux rose above baseline.

In the following analysis, we focus on the TC-7020 response and disregard the nicotine response, which was generated by identical mechanisms (activation of α4β2 NNRs) in both models alike.

The effect of agonist concentration

Because the drop in dopamine release was generated in the activation model by a window NNR current (in the GABA neuron's afferents), lower TC-7020 doses were needed (peak concentrations from 0.8 to 15 nM; Fig. S4 A, right) than in the desensitization model (from 4 to 37 nM in the left panel of Fig. S4 A). In both models, dopamine efflux dropped faster at higher doses of TC-7020, a consequence of accelerated desensitization and activation, reflecting the nonlinearity of reaction kinetics (see also the current traces in Fig. S1). The depth of the drop was also dose-dependent, but was bounded in the desensitization model, where a substantial tonic α4β2* component contributed to baseline dopamine release. The activation model, in contrast, was not able to maintain the drop in dopamine release at high doses of TC-7020 (Fig. S4 A, right, black curve) because the α7 NNRs on the afferents to the GABA neurons started to desensitize after a few seconds, disinhibiting the dopamine neurons.

The effect of agonist efficacy

A distinguishing feature between the models is that in the desensitization model a full α7 agonist evoked a transient peak before the dopamine efflux dropped (Fig. S4 B,

left panel). In contrast, a full agonist caused dopamine concentration only to drop faster and deeper in the activation model without evoking an intial peak (Fig. S4 B, right). In constructing these curves, we assumed that all agonists desensitized the α7 NNR to the same degree, irrespective of their efficacy (*2-4*). This assumption can be made, since α7 ligands show a poor correlation between activation and residual inhibition or desensitization (M. Bencherif, unpublished data). We also simulated efficacies higher than those reported for currents recorded in vitro (> 100%), because the presence of a receptor reserve may enhance the physiological efficacy in vivo (*5*). NNRs of the α7 type in particular have been suggested to prolong responses by buffering spilled-over acetylcholine (*6, 7*).

The effect of co-administration of PNU-120596

PNU-120596 is a type-2 positive allosteric modulator of α7 NNRs, releasing the receptors from desensitization (*8*). We modelled this effect by shifting the Hill-curve of the desensitization gate towards higher agonist concentrations, leaving the activation gate unchanged. (Positive allosteric modulators of type 2 also shift the activation gate, but this effect is compensated by a concomitantly enhanced endogenous activation by acetylcholine and choline, which enhances the cholinergic tone and partly reduces the net effect of the agonist, see Fig. 5.) In that case, the desensitization model robustly reproduced the experimental cancellation of the TC-7020-induced drop in dopamine release (Fig. S4 C, left panel). The combined administration of ortho- and allosteric compound could even slightly enhance dopamine release, an effect that was readily suppressed by enhancing the cholinergic tone (compare blue and black curves in Fig. S4 C, left).

In the activation model, in contrast, rightward shifting the desensitization curves always amplified the TC-7020 response, instead of neutralizing it (Fig. S4 C, right panel). For the TC-7020 response to be cancelled in the activation model, PNU-120596 should be assumed to interfere with receptor activation, or to block the channel.

The effect of allosteric agonists

Some recently studied allosteric modulators such as 4BP-TSQ, or its (+) enantiomer GAT107, have intrinsic (allosteric) agonist activity (*9, 10*). Simulating these compounds made the strongest model predictions, as they amplified the drop in

dopamine release in the activation model (Fig. S4 D, red curve right panel), but reversed the drop into a genuine dopamine efflux in the desensitization model (Fig. S4 D, red curve left, see legend for details).

Can α7 ligands potentiate the receptor response through co-agonism with acetylcholine?

As an alternative to receptor desensitization and activation, some partial agonists such as EVP-6124 have been suggested to act through co-agonism with endogenous acetylcholine (*11*). EVP-6124 would enhance the effect of endogenous acetylcholine at brain concentrations lower than those needed for desensitization or activation. The mechanism involves channel opening after paired binding of one acetylcholine molecule and one molecule of partial agonist at the two available binding sites. In the formulas for receptor occupancy these cross-terms between different ligands are commonly neglected, either because such configurations are very transient or because they do not open the channel. They may, however, explain some of the potentiation effects observed at low concentrations of agonists or antagonists (*12, 13*).

In the simulations presented below, channel current was calculated using the ad hoc formula

$$\frac{w_x x^{n_x} + 2w_{xy} xy + w_y y^{n_y}}{1 + x^{n_x} + 2xy + y^{n_y} + 2x + 2y}$$

where x and y, representing ACh and TC-7020, are the normalized concentrations (concentration divided by the respective EC_{50}, or DC_{50}), the n's Hill coefficients and the w's weight factors. Note that this formula is identical to the formula derived by Cachelin and Rust (*12*) for the potentiating effect of an antagonist (w_y=0), provided the receptor has two non-cooperating binding sites (n_x=n_y=2). As before, parameters were set to the values given in Table 1, except for the new free parameter w_{xy}, which expressed the efficacy of channel opening (or desensitization) by co-agonist receptor binding.

We calculated the α7 current to trains of 5-s puffs of acetylcholine, in the presence of varying concentrations of an α7 compound (Figure S5). We first examined this co-agonist mechanism for a competitive antagonist (Fig. S5 A), using as ligand TC-7020 but with zero efficacy and without allowing either acetylcholine or TC-7020 to desensitize the receptor. As in Smulders et al. (*14*), continuous application of a low dose of antagonist potentiated the responses to puffs of 1 μM acetylcholine. With w_{xy} = 0.3 at the activation gate, the response increased by 37% (upper panel in Fig. S5 A). As in Smulders et al., however, potentiation failed when higher doses of acetylcholine were used (lower panel).

We next tried to replicate, using TC-7020 at its 30% efficacy, the observations which Prickaerts et al. (*11*) made with the partial agonist EVP-6124 (a sequence of potentiation of the puff response, suppression by desensitization, and opening of the channel by the agonist itself). EVP-6124, however, has a very high EC_{50}/DC_{50} ratio, and in order to obtain desensitization in the absence of overt activation, the EC_{50} for TC-7020 had to be increased from 30 to 300 nM. Even so, a cross-term weight of w_{xy} = 20 at the activation gate gave less than 9% potentiation. If, in contrast, puffed acetylcholine was allowed to desensitize the receptor (DC_{50} = 1.3 μM) in this in vitro condition (absence of cholinesterase), potentiation was readily obtained (Fig. S5 B). It sufficed to set the cross-term weight w_{xy} to zero at the desensitization gate (and at the activation gate as well) to obtain a potentiation of 55% (upper panel in Fig. S5 B). Note that this zero cross-term implied that the co-agonist pair did not desensitize the receptor, whereas each ligand in itself did. Hence, the underlying mechanism is competitive inhibition of the co-agonist pair with pairs of identical ligands, protecting the receptor from desensitization. Note also that the further increase in amplitude after a 60-s interval at 480 s is due to a partial recovery from desensitization. When the partial agonist was applied at higher concentrations (lower panel in Fig. S5 B), desensitization overruled co-agonist potentiation and the response dropped during agonist infusion. At still higher concentrations, the partial agonist caused channel opening on its own and the baseline between puffs rose (not shown).

Although a full study of this mechanism is beyond the scope of the present manuscript, the present results show that there may be a narrow range of concentrations of both acetylcholine and partial agonist at which these ligands would cooperate, as in Fig. S5 A. As for the in vitro experiment, our results suggest that the

potentiation effect is a consequence of reduced desensitization rather than enhanced activation.

Supplementary discussion

Mesocortical versus mesolimbic dopamine release

Can the present desensitization model for the accumbal action of α7 partial agonists be extrapolated to other systems such as prefrontal cortex, where NNRs are also abundantly expressed (*15*)? This is an important question because α7 ligands such as AZD0328 (*16-18*), EVP-6124 (*11*), RG3487 (*19*) and JN403 (*20*) have been reported to generate positive cognitive effects at low nanomolar or subnanomolar plasma concentrations (although for JN403 the brain concentration was reported to be higher than its EC_{50} value). α7 NNR knock-out mice, in turn, show deficits in attention and memory (*21*). The pro-cognitive action of α7 ligands has been ascribed to receptor activation (*16, 19, 20, 22*), receptor desensitization (*2, 23*), receptor antagonism (*24*) or to potentiation of the receptor's response to endogenous acetylcholine (*10, 11*). Moreover, α7 NNRs have been suggested to be able to exert an effect via intracellular signalling mechanisms, even when they are in a nonconducting (desensitized but strongly agonist-binding) state (*25, 26*), and in the long run, compensatory mechanisms may come into play, such as up- or downregulation of receptors subtypes (*27*), and changes in circuit connectivity as a consequence of synaptic plasticity.

According to the model, the acute effects will be determined by ligand-specific and circuit-specific characteristics. Ligand-specific characteristics include, apart from differences in the efficacies to activate and desensitize the receptor and in the amplitude of the window current, also cross-affinities for other receptors. The partial agonist EVP-6124, for instance, is also a functional antagonist of 5-HT_3 receptors (*11*), through which it may enhance the release of acetylcholine and, secondarily, dopamine (*28*).

The most important circuit characteristics are the distribution of α7 NNRs over principal neurons versus interneurons and the level of the cholinergic tone. There were two mechanisms through which a partial agonist could *enhance* dopamine efflux in the model. The first one is the desensitization of α7 NNRs positioned primarily on GABAergic neurons or afferents to them. Indeed, a distribution value *s* less than 0.6 (> 40% of receptors on GABA-neurons or their afferents) would reverse the drop in [dopamine] in Figs. 2 and S2 (left column) into a [dopamine] rise, at least in the presence of a cholinergic tone. The second mechanism is activation of α7 NNRs

positioned primarily on dopamine neurons or afferents to them, in the absence of cholinergic tone (curve labeled 'ACh 0' in Fig. 2B).

Both these circuit characteristics (tone and receptor distribution) may differ between nucleus accumbens and prefrontal cortex. Whereas α7 NNRs are sparse or absent on accumbal interneurons (*29, 30*), they are richly expressed on most inhibitory neurons of mouse prefrontal cortex (*15*) and hippocampus. In addition, whereas the cholinergic tone in nucleus accumbens is determined by intrinsic interneurons (*31*), prefrontal cortex receives projections from telencephalic basal nuclei, and its cholinergic tone may fluctuate significantly, from very low during slow-wave sleep to high during attention and REM sleep. As noted above and shown in Fig. 5, a low tone will accentuate α7 activation, whereas the window for activation will be narrower and shift to lower agonist concentrations when the tone increases.

No cyclic voltammetry data are availabale for prefrontal cortex because dopamine signals may be contaminated by noradrenaline, as prefrontal cortex, unlike the basal ganglia, receives a rich innervation from locus coeruleus (*32*). α7 agonists applied to prefrontal cortex through reverse dialysis, however, were found to evoke dopamine release in anaeshetized rats (*33, 34*), and this release was enhanced by systemical or local application of PNU-120596 (*33*). From the failure of local PNU-120596 to raise dopamine on its own in anaesthetized animals, Livingstone et al. (*33, 35*) concluded the endogenous cholinergic tone to be lower in prefrontal cortex than in the basal ganglia. Note that our desensitization model, which generated a drop in dopamine release in the presence of a high cholinergic tone, also generated dopamine efflux when the tone was low or absent (blue curve in Fig. 2B). In accordance with this, only very small doses of an α7 partial agonist, systemically applied in awake cats, were able to enhance dopamine release in the prefrontal cortex (*17*); and in behaving monkeys, only low doses of iontophoretically applied agonist enhanced persistent firing in pyramidal cells (*18*).

To further speculate on this, we suggest that α7 agonists act by activating NNRs when the cholinergic tone is low. For instance, memory consolidation in hippocampus is known to require a low cholinergic tone (*36*) and under such conditions preterminal α7 NNRs may promote synaptic plasticty (*37-40*). At higher cholinergic tone, such as that observed during attention, α7 agonists may act by desensitizing NNRs, and hence for instance sharpening the cholinergic transients thought to improve attential performance (*6, 41*).

Supplementary figure legends

Figure S1. Concentration-response curves for activation and desensitization of model NNRs.

Fraction of NNRs that are at steady-state in the sensitive (gray curves) and active state (black) for the following compound-receptor interactions: the action of TC-7020 on α7 NNRs (A), nicotine on α7 NNRs (B) and nicotine on α4β2 NNRs (C). Note that the activation curves are plotted full-scale; the actual efficacies relative to acetylcholine are 0.3, 0.8 and 0.8 respectively (Table 1). Above the dose-response curves, time traces of receptor current are drawn for varying concentrations; the relative amplitudes of the currents are indicated by the heights of the corresponding color bars on the dose-response graphs.

Figure S2. Deconstruction of the responses of the desensitization (left) and activation models (right) to TC-7020 and nicotine, administered at 30 s and 60 s respectively (bottom arrows and vertical guide lines). A. Dopamine concentration (nM) in nucleus accumbens (black). The gray traces were calculated with a slower (left) or faster (right) brain-availability of TC-7020 than used in the standard simulations of each model, and correspond to the gray concentration profiles in E. B. Population activities of dopamine (DA) (black) and GABA neurons (red) in the VTA (using arbitrary units). C. Fraction of conducting channels for NNRs of the α7 (blue) and α4β2∗ subtypes (green) (traces identical for DA and GABA neurons). Note that in the right panel the left vertical axis plots α7 opening, the right axis α4β2∗ opening. D, E. Time-courses of the concentrations of nicotine (D) and TC-7020 (E).

Figure S3. The effect of varying cholinergic tone on dopamine release in the desensitization (A) and activation model (B). TC-7020 and nicotine were applied as described in Fig. S2. The insets show the responses of the dopamine neuron in the desensitization model (A) and the GABA neuron in the activation model (B). Tones are expressed as equivalent constant background concentrations (μM) of acetylcholine (ACh). Note that the cholinergic tone determines the baseline levels of activity in the insets, but that this effect has been normalized in the dopamine plots as described in Methods.

Figure S4. Comparative analysis of dopamine release in the desensitization (left column) and activation model (right). As before, TC-7020 and nicotine were applied at 30 s and 60 s, respectively. Since the nicotine response was largely invariant, only the TC-7020 response is shown. A. Effect of varying TC-7020 concentration (peak values given in legend). B. Effect of varying the efficacy of the α7 agonist, for peak agonist concentrations of 11 nM in the desensitization model and 3.9 nM in the activation model. C and D. Effects of applying positive allosteric modulators (PAM) in the model. C. The dose at which the α7 receptor is half-maximally desensitized (DC_{50}) was varied, using the same agonist concentrations as in B. The values in the legend give the factor by which the steady-state desensitization curve was shifted to the right. The black trace on the left used a cholinergic tone of 30 instead of 20 μM. D. The blue traces are the controls using TC-7020. The green traces had the sensitization gate clamped at unity (modeling complete resensitization by a type-2 PAM). Red traces had in addition the efficacy raised to 100%, modelling the putative effect of a PAM with intrinsic agonist activity ("ago-PAM").

Figure S5. Co-agonist potentiation at the model α7 NNR. Pulses of acetylcholine of 5 s duration were applied at regular intervals (arrows), before, during and after the application of a competitive agonist (A) or a partial agonist (B) (horizontal bars). A. The antagonist potentiates the response to pulses of 10 μM acetylcholine (upper trace), but not to 60 μM pulses (lower trace). Parameters as for TC-7020 but with zero efficacy, and a co-agonist cross-term weight w_{xy} = 0.3 at the activation gate. Neither acetylcholine nor the antagonist were allowed to desensitize the receptor. B. A low dose of partial agonist (upper trace) potentiates the response to pulses of 60 μM acetylcholine, whereas a higher dose of partial agonist (lower trace) suppresses the responses through desensitization. Parameters as for TC-7020 (30 % efficay), but the EC_{50} had been increased by a factor of 10 (from 30 to 300 nM), as described in the text. Both the partial agonist and acetylcholine were allowed to desensitize the receptor, and the cross-term weight w_{xy} was set to zero at both the activation and desensitization gate.

Supplementary references

1. Brewer, B. G., Roberts, A. M., and Rowell, P. P. (2004) Short-term distribution of nicotine in the rat lung. *Drug Alcohol Depend. 75*, 193-198.
2. Buccafusco, J. J., Shuster, L. C., and Terry, A. V., Jr. (2007) Disconnection between activation and desensitization of autonomic nicotinic receptors by nicotine and cotinine. *Neurosci. Lett. 413*, 68-71.
3. Wang, J., Horenstein, N. A., Stokes, C., and Papke, R. L. (2010) Tethered agonist analogs as site-specific probes for domains of the human *α*7 nicotinic acetylcholine receptor that differentially regulate activation and desensitization. *Mol. Pharmacol. 78*, 1012-1025.
4. Charlton, S. J. (2009) Agonist efficacy and receptor desensitization: from partial truths to a fuller picture. *Br. J. Pharmacol. 158*, 165-168.
5. Chen, Y., Broad, L. M., Phillips, K. G., and Zwart, R. (2012) Partial agonists for α4β2 nicotinic receptors stimulate dopaminergic neuron firing with relatively enhanced maximal effects. *Br. J. Pharmacol. 165*, 1006-1016.
6. Parikh, V., Ji, J., Decker, M. W., and Sarter, M. (2010) Prefrontal β2 subunit-containing and α7 nicotinic acetylcholine receptors differentially control glutamatergic and cholinergic signaling. *J. Neurosci. 30*, 3518-3530.
7. Stanchev, D., and Sargent, P. B. (2011) α7-Containing and non-α7-containing nicotinic receptors respond differently to spillover of acetylcholine. *J. Neurosci. 31*, 14920-14930.
8. Hurst, R. S., Hajós, M., Raggenbass, M., Wall, T. M., Higdon, N. R., Lawson, J. A., Rutherford-Root, K. L., Berkenpas, M. B., Hoffmann, W. E., Piotrowski, D. W., Groppi, V. E., Allaman, G., Ogier, R., Bertrand, S., Bertrand, D., and Arneric, S. P. (2005) A novel positive allosteric modulator of the α7 neuronal nicotinic acetylcholine receptor: *in vitro* and *in vivo* characterization. *J. Neurosci. 25*, 4396-4405.
9. Gill, J. K., Savolainen, M., Young, G. T., Zwart, R., Sher, E., and Millar, N. S. (2011) Agonist activation of α7 nicotinic acetylcholine receptors via an allosteric transmembrane site. *Proc. Natl. Acad. Sci. U. S. A. 108*, 5867-5872.
10. Papke, R. L., Horenstein, N. A., Kulkarni, A. R., Stokes, C., Corrie, L. W., Maeng, C. Y., and Thakur, G. A. (2014) The activity of GAT107, an allosteric activator and positive modulator of α7 nicotinic acetylcholine receptors (nAChR), Is regulated by aromatic amino acids that span the subunit interface. *J. Biol. Chem. 289*, 4515-4531.
11. Prickaerts, J., van Goethem, N. P., Chesworth, R., Shapiro, G., Boess, F. G., Methfessel, C., Reneerkens, O. A., Flood, D. G., Hilt, D., Gawryl, M., Bertrand, S., Bertrand, D., and König, G. (2012) EVP-6124, a novel and selective *α*7 nicotinic acetylcholine receptor partial agonist, improves memory performance by potentiating the acetylcholine response of *α*7 nicotinic acetylcholine receptors. *Neuropharmacology 62*, 1099-1110.
12. Cachelin, A. B., and Rust, G. (1994) Unusual pharmacology of (+)-tubocurarine with rat neuronal nicotinic acetylcholine receptors containing beta 4 subunits. *Mol. Pharmacol. 46*, 1168-1174.
13. Zwart, R., and Vijverberg, H. P. (1997) Potentiation and inhibition of neuronal nicotinic receptors by atropine: competitive and noncompetitive effects. *Mol. Pharmacol. 52*, 886-895.
14. Smulders, C. J., Zwart, R., Bermudez, I., van Kleef, R. G., Groot-Kormelink, P. J., and Vijverberg, H. P. (2005) Cholinergic drugs potentiate human

nicotinic α4β2 acetylcholine receptors by a competitive mechanism. *Eur. J. Pharmacol. 509*, 97-108.

15. Poorthuis, R. B., Bloem, B., Schak, B., Wester, J., de Kock, C. P., and Mansvelder, H. D. (2013) Layer-specific modulation of the prefrontal cortex by nicotinic acetylcholine receptors. *Cereb. Cortex 23*, 148-161.
16. Castner, S. A., Smagin, G. N., Piser, T. M., Wang, Y., Smith, J. S., Christian, E. P., Mrzljak, L., and Williams, G. V. (2011) Immediate and sustained improvements in working memory after selective stimulation of α7 nicotinic acetylcholine receptors. *Biol. Psychiatry 69*, 12-18.
17. Sydserff, S., Sutton, E. J., Song, D., Quirk, M. C., Maciag, C., Li, C., Jonak, G., Gurley, D., Gordon, J. C., Christian, E. P., Doherty, J. J., Hudzik, T., Johnson, E., Mrzljak, L., Piser, T., Smagin, G. N., Wang, Y., Widzowski, D., and Smith, J. S. (2009) Selective α7 nicotinic receptor activation by AZD0328 enhances cortical dopamine release and improves learning and attentional processes. *Biochem. Pharmacol. 78*, 880-888.
18. Yang, Y., Paspalas, C. D., Jin, L. E., Picciotto, M. R., Arnsten, A. F., and Wang, M. (2013) Nicotinic α7 receptors enhance NMDA cognitive circuits in dorsolateral prefrontal cortex. *Proc. Natl. Acad. Sci. U. S. A. 110*, 12078-12083.
19. Wallace, T. L., Callahan, P. M., Tehim, A., Bertrand, D., Tombaugh, G., Wang, S., Xie, W., Rowe, W. B., Ong, V., Graham, E., Terry, A. V., Jr., Rodefer, J. S., Herbert, B., Murray, M., Porter, R., Santarelli, L., and Lowe, D. A. (2011) RG3487, a novel nicotinic α7 receptor partial agonist, improves cognition and sensorimotor gating in rodents. *J. Pharmacol. Exp. Ther. 336*, 242-253.
20. Feuerbach, D., Lingenhoehl, K., Olpe, H. R., Vassout, A., Gentsch, C., Chaperon, F., Nozulak, J., Enz, A., Bilbe, G., McAllister, K., and Hoyer, D. (2009) The selective nicotinic acetylcholine receptor α7 agonist JN403 is active in animal models of cognition, sensory gating, epilepsy and pain. *Neuropharmacology 56*, 254-263.
21. Leiser, S. C., Bowlby, M. R., Comery, T. A., and Dunlop, J. (2009) A cog in cognition: how the alpha 7 nicotinic acetylcholine receptor is geared towards improving cognitive deficits. *Pharmacol. Ther. 122*, 302-311.
22. Briggs, C. A., Grønlien, J. H., Curzon, P., Timmermann, D. B., Ween, H., Thorin-Hagene, K., Kerr, P., Anderson, D. J., Malysz, J., Dyhring, T., Olsen, G. M., Peters, D., Bunnelle, W. H., and Gopalakrishnan, M. (2009) Role of channel activation in cognitive enhancement mediated by α7 nicotinic acetylcholine receptors. *Br. J. Pharmacol. 158*, 1486-1494.
23. Buccafusco, J. J., Beach, J. W., and Terry, A. V., Jr. (2009) Desensitization of nicotinic acetylcholine receptors as a strategy for drug development. *J. Pharmacol. Exp. Ther. 328*, 364-370.
24. Levin, E. D., Cauley, M., and Rezvani, A. H. (2013) Improvement of attentional function with antagonism of nicotinic receptors in female rats. *Eur. J. Pharmacol. 702*, 269-274.
25. Skok, M. V. (2009) Editorial: To channel or not to channel? Functioning of nicotinic acetylcholine receptors in leukocytes. *J. Leukoc. Biol. 86*, 1-3.
26. Williams, D. K., Wang, J., and Papke, R. L. (2011) Investigation of the molecular mechanism of the *α*7 nicotinic acetylcholine receptor positive allosteric modulator PNU-120596 provides evidence for two distinct desensitized states. *Mol. Pharmacol. 80*, 1013-1032.

27. Melis, M., Scheggi, S., Carta, G., Madeddu, C., Lecca, S., Luchicchi, A., Cadeddu, F., Frau, R., Fattore, L., Fadda, P., Ennas, M. G., Castelli, M. P., Fratta, W., Schilstrom, B., Banni, S., De Montis, M. G., and Pistis, M. (2013) PPARα regulates cholinergic-driven activity of midbrain dopamine neurons via a novel mechanism involving α7 nicotinic acetylcholine receptors. *J. Neurosci. 33*, 6203-6211.
28. Huang, M., Felix, A. R., Flood, D. G., Bhuvaneswaran, C., Hilt, D., Koenig, G., and Meltzer, H. Y. (2014) The novel alpha7 nicotinic acetylcholine receptor agonist EVP-6124 enhances dopamine, acetylcholine, and glutamate efflux in rat cortex and nucleus accumbens. *Psychopharmacology*, DOI 10.1007/s00213-00014-03596-00210.
29. Klink, R., de Kerchove d'Exaerde, A., Zoli, M., and Changeux, J. P. (2001) Molecular and physiological diversity of nicotinic acetylcholine receptors in the midbrain dopaminergic nuclei. *J. Neurosci. 21*, 1452-1463.
30. Taylor, D. H., Burman, P. N., Hansen, M. D., Wlcox, R. S., Larsen, B. R., Blanchard, J. K., Merrill, C. B., Edwards, J. G., Sudweeks, S. N., Jie Wu, M. D., Arias, H. R., and Steffensen, S. C. (2013) Nicotine enhances the excitability of Gaba neurons in the ventral tegmental area via activation of alpha 7 nicotinic receptors on glutamate terminals. *Biochem. & Pharmacol. S1*, 007.
31. Goldberg, J. A., and Reynolds, J. N. (2011) Spontaneous firing and evoked pauses in the tonically active cholinergic interneurons of the striatum. *Neuroscience 198*, 27-43.
32. Briand, L. A., Gritton, H., Howe, W. M., Young, D. A., and Sarter, M. (2007) Modulators in concert for cognition: modulator interactions in the prefrontal cortex. *Prog. Neurobiol. 83*, 69-91.
33. Livingstone, P. D., Srinivasan, J., Kew, J. N., Dawson, L. A., Gotti, C., Moretti, M., Shoaib, M., and Wonnacott, S. (2009) α7 and non-α7 nicotinic acetylcholine receptors modulate dopamine release *in vitro* and *in vivo* in the rat prefrontal cortex. *Eur. J. Neurosci. 29*, 539-550.
34. Wu, J., Khan, G. M., and Nichols, R. A. (2007) Dopamine release in prefrontal cortex in response to β-amyloid activation of α7* nicotinic receptors. *Brain Res. 1182*, 82-89.
35. Livingstone, P. D., Dickinson, J. A., Srinivasan, J., Kew, J. N., and Wonnacott, S. (2010) Glutamate-dopamine crosstalk in the rat prefrontal cortex is modulated by alpha7 nicotinic receptors and potentiated by PNU-120596. *J. Mol. Neurosci. 40*, 172-176.
36. Gais, S., and Born, J. (2004) Low acetylcholine during slow-wave sleep is critical for declarative memory consolidation. *Proc. Natl. Acad. Sci. U. S. A. 101*, 2140-2144.
37. Ondrejcak, T., Wang, Q., Kew, J. N., Virley, D. J., Upton, N., Anwyl, R., and Rowan, M. J. (2012) Activation of α7 nicotinic acetylcholine receptors persistently enhances hippocampal synaptic transmission and prevents Aβ-mediated inhibition of LTP in the rat hippocampus. *Eur. J. Pharmacol. 677*, 63-70.
38. Lin, H., Vicini, S., Hsu, F. C., Doshi, S., Takano, H., Coulter, D. A., and Lynch, D. R. (2010) Axonal α7 nicotinic ACh receptors modulate presynaptic NMDA receptor expression and structural plasticity of glutamatergic presynaptic boutons. *Proc. Natl. Acad. Sci. U. S. A. 107*, 16661-16666.

39. Halff, A. W., Gomez-Varela, D., John, D., and Berg, D. K. (2014) A novel mechanism for nicotinic potentiation of glutamatergic synapses. *J. Neurosci. 34*, 2051-2064.
40. Wang, X., Lippi, G., Carlson, D. M., and Berg, D. K. (2013) Activation of α7-containing nicotinic receptors on astrocytes triggers AMPA receptor recruitment to glutamatergic synapses. *J. Neurochem. 127*, 632-643.
41. Howe, W. M., Ji, J., Parikh, V., Williams, S., Mocaër, E., Trocmé-Thibierge, C., and Sarter, M. (2010) Enhancement of attentional performance by selective stimulation of α4β2* nAChRs: underlying cholinergic mechanisms. *Neuropsychopharmacology 35*, 1391-1401.

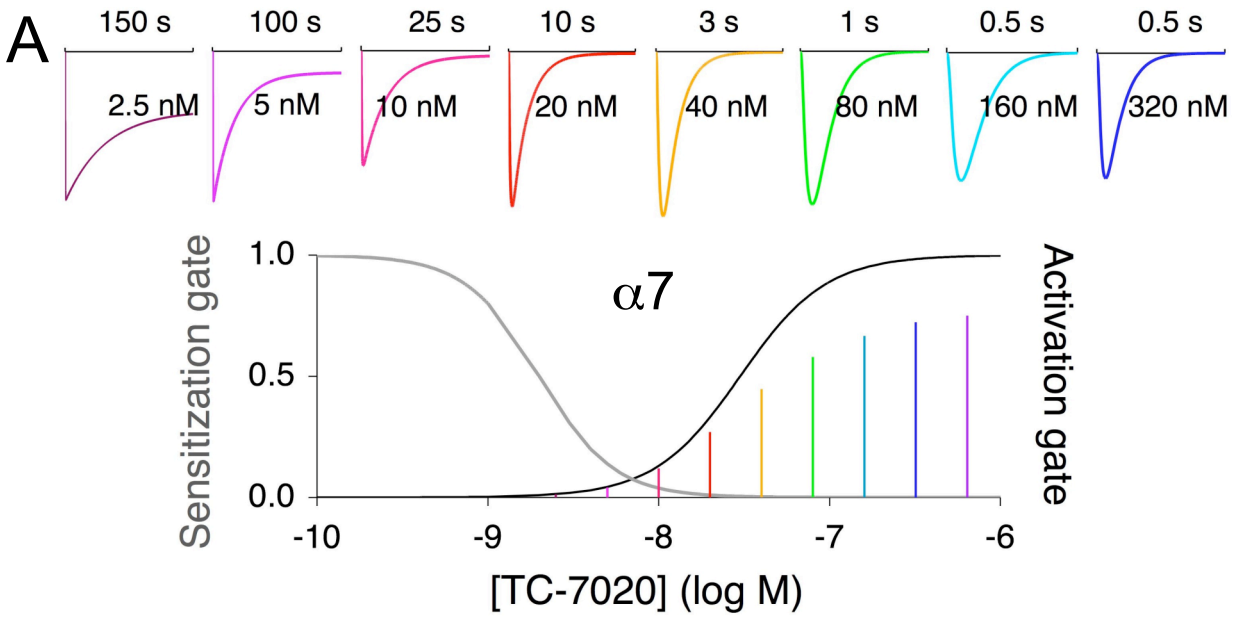
A
150 s
100 s
25 s
10 s
3 s
1 s
0.5 s
0.5 s
2.5 nM
5 nM
10 nM
20 nM
40 nM
80 nM
160 nM
320 nM
Sensitization gate
Activation gate
α7
1.0
0.5
0.0
-10
-9
-8
-7
-6
[TC-7020] (log M)

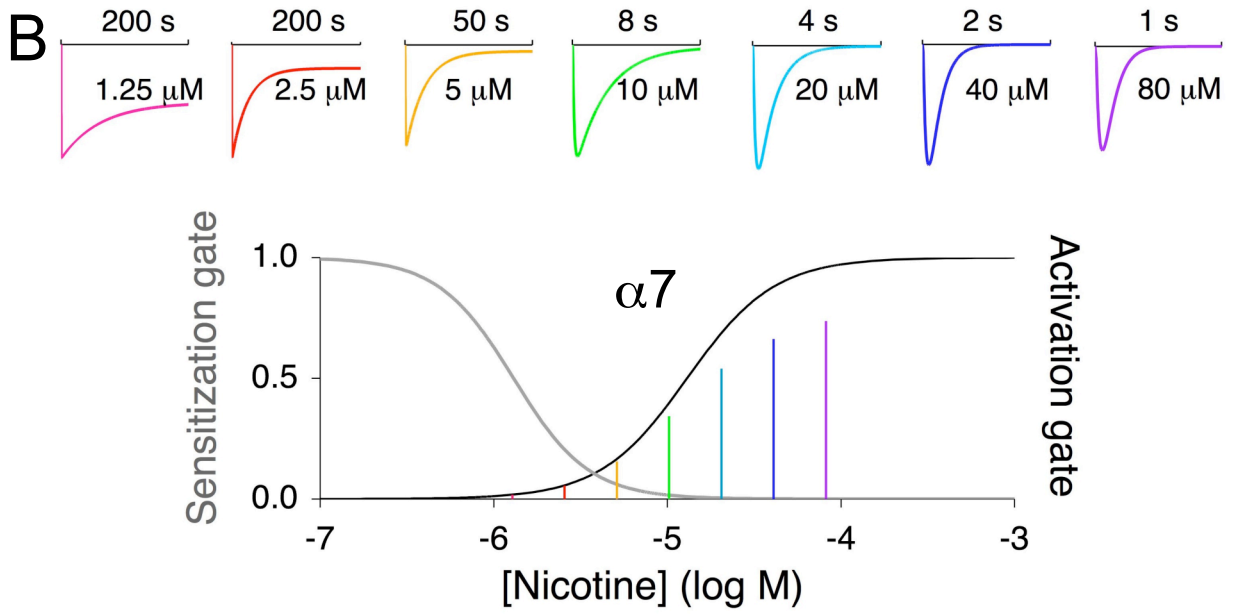
B
200 s
200 s
50 s
8 s
4 s
2 s
1 s
1.25 μM
2.5 μM
5 μM
10 μM
20 μM
40 μM
80 μM
Sensitization gate
Activation gate
α7
1.0
0.5
0.0
-7
-6
-5
-4
-3
[Nicotine] (log M)

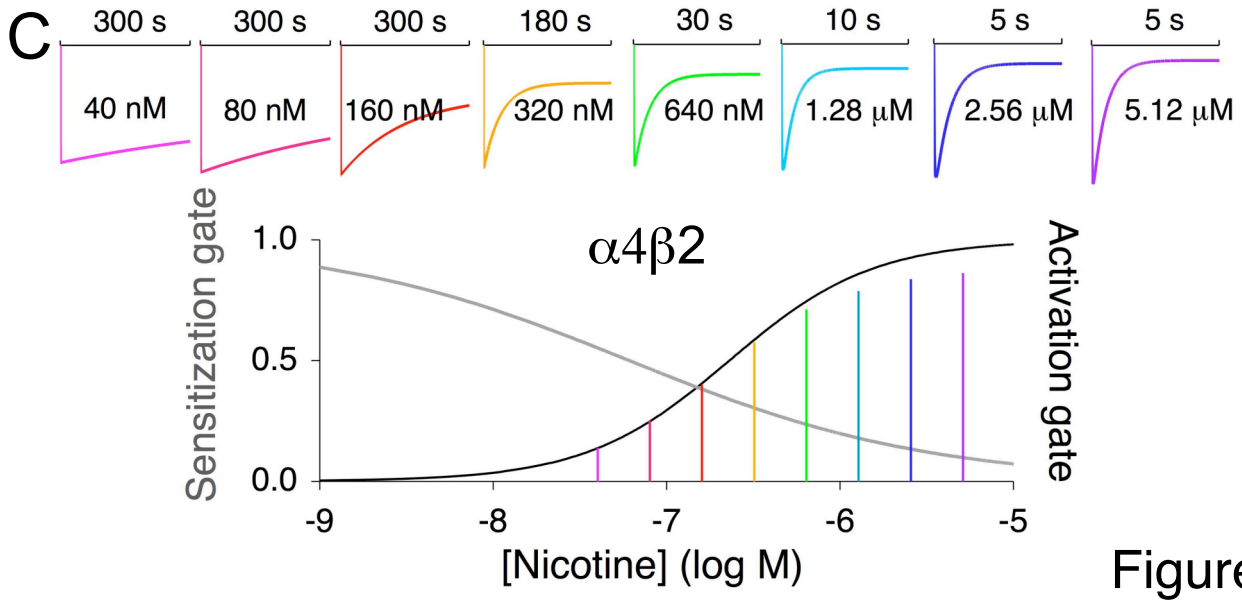
C
300 s
300 s
300 s
180 s
30 s
10 s
5 s
5 s
40 nM
80 nM
160 nM
320 nM
640 nM
1.28 μM
2.56 μM
5.12 μM
Sensitization gate
Activation gate
α4β2
1.0
0.5
0.0
-9
-8
-7
-6
-5
[Nicotine] (log M)

Figure S1

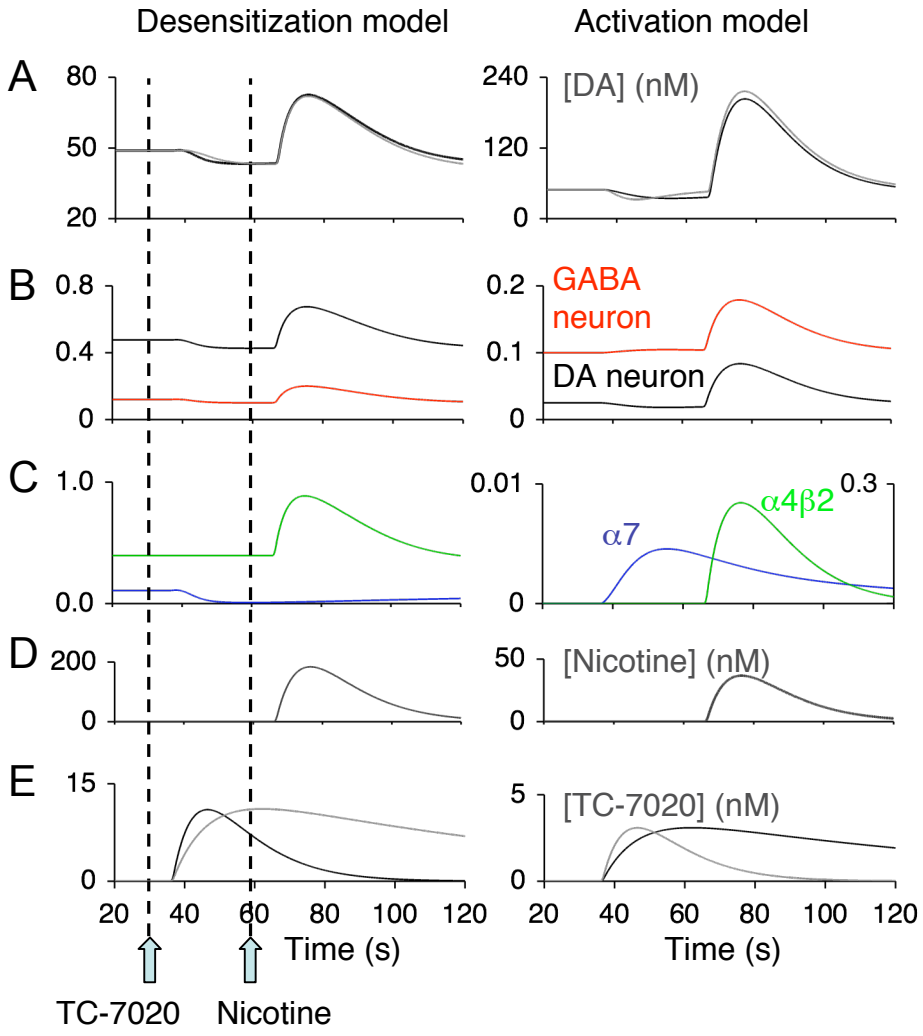
Desensitization model
Activation model
A
80
50
20
240
120
0
[DA] (nM)
B
0.8
0.4
0
0.2
0.1
0
GABA
neuron
DA neuron
C
1.0
0.0
0.01
0
0.3
α7
α4β2
D
200
0
50
0
[Nicotine] (nM)
E
15
0
5
0
[TC-7020] (nM)
20
40
60
80
100
120
Time (s)
TC-7020
Nicotine

Figure S2

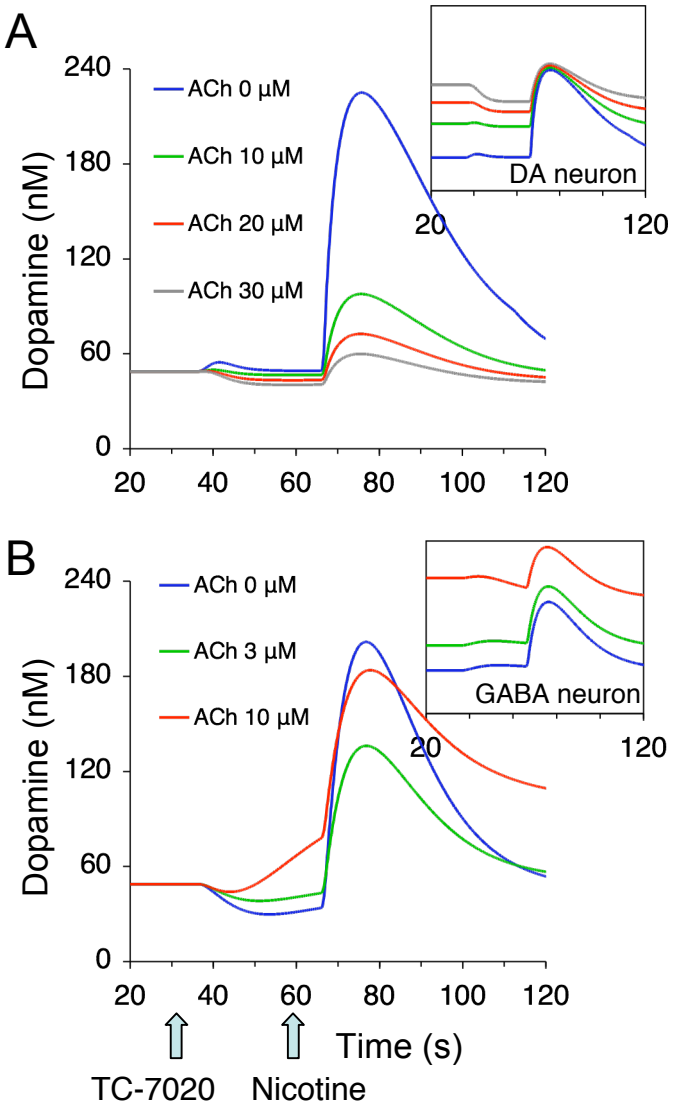
A
240
180
120
60
0
Dopamine (nM)
ACh 0 μM
ACh 10 μM
ACh 20 μM
ACh 30 μM
DA neuron
20
120
20
40
60
80
100
120
B
240
180
120
60
0
Dopamine (nM)
ACh 0 μM
ACh 3 μM
ACh 10 μM
GABA neuron
20
120
20
40
60
80
100
120
Time (s)
TC-7020
Nicotine

Figure S3

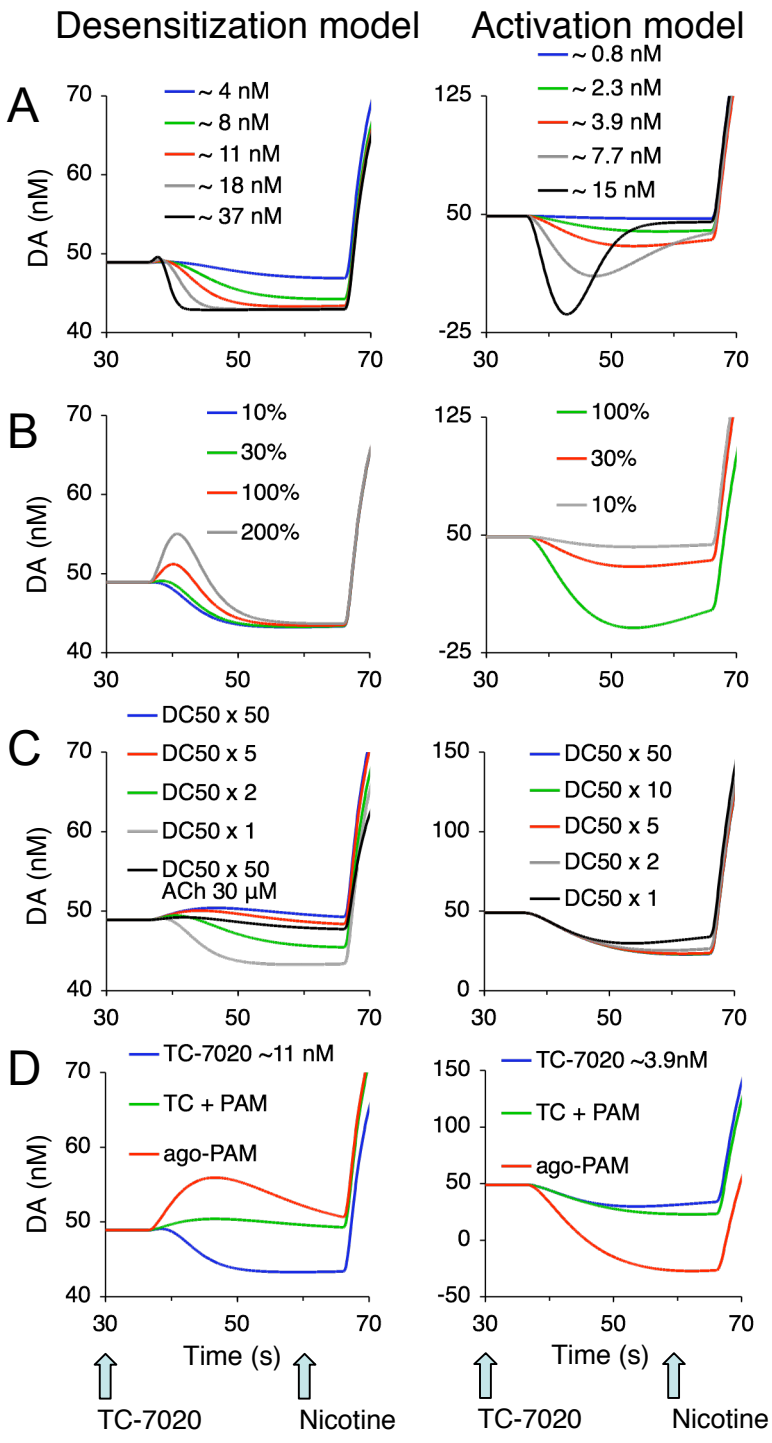
Desensitization model
Activation model
A
B
C
D
DA (nM)
~ 4 nM
~ 8 nM
~ 11 nM
~ 18 nM
~ 37 nM
~ 0.8 nM
~ 2.3 nM
~ 3.9 nM
~ 7.7 nM
~ 15 nM
10%
30%
100%
200%
DC50 x 50
DC50 x 5
DC50 x 2
DC50 x 1
DC50 x 50
ACh 30 µM
DC50 x 10
TC-7020 ~11 nM
TC + PAM
ago-PAM
TC-7020 ~3.9nM
Time (s)
TC-7020
Nicotine

Figure S4

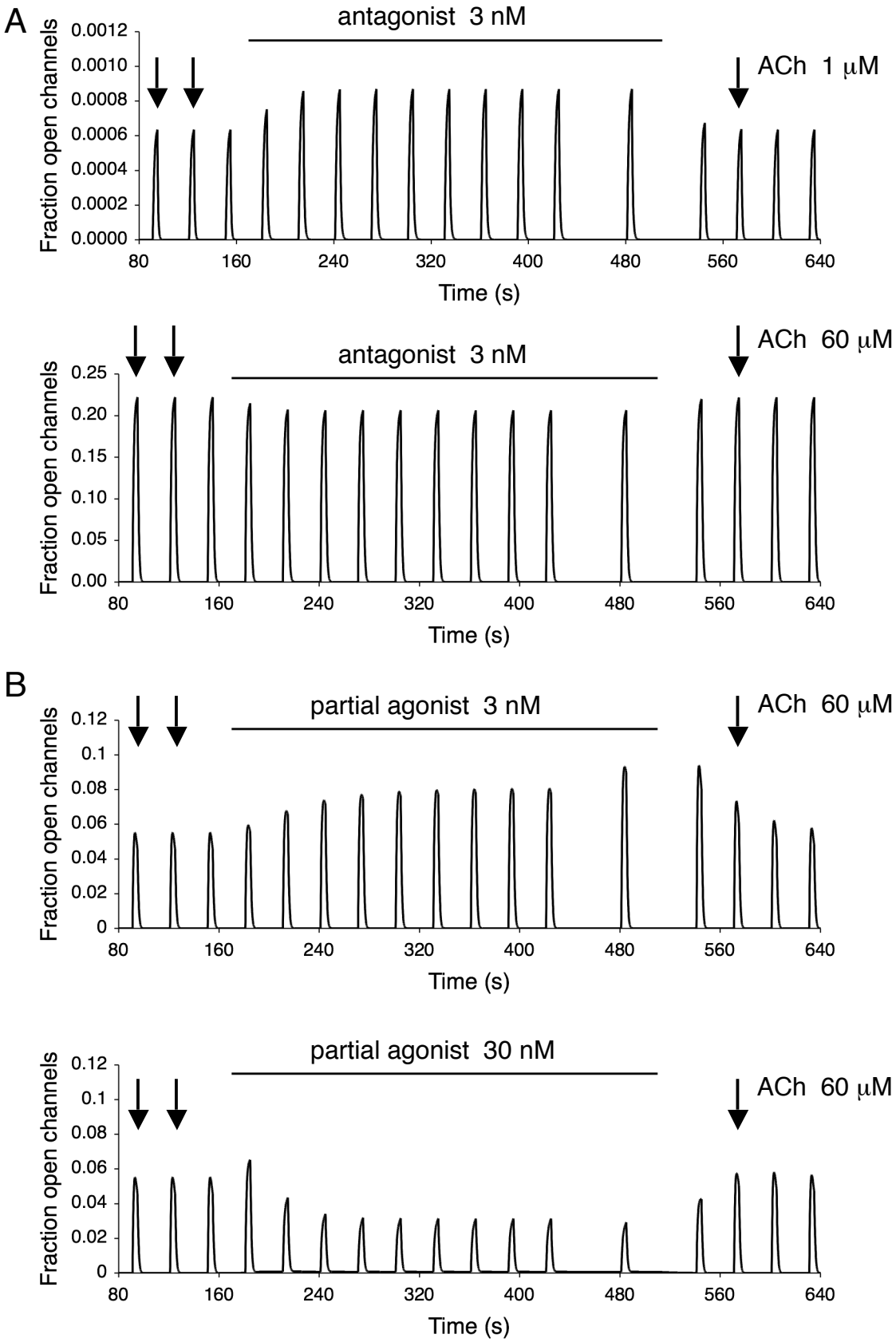
A
antagonist 3 nM
ACh 1 μM
Fraction open channels
0.0012
0.0010
0.0008
0.0006
0.0004
0.0002
0.0000
80
160
240
320
400
480
560
640
Time (s)
antagonist 3 nM
ACh 60 μM
Fraction open channels
0.25
0.20
0.15
0.10
0.05
0.00
80
160
240
320
400
480
560
640
Time (s)
B
partial agonist 3 nM
ACh 60 μM
Fraction open channels
0.12
0.1
0.08
0.06
0.04
0.02
0
80
160
240
320
400
480
560
640
Time (s)
partial agonist 30 nM
ACh 60 μM
Fraction open channels
0.12
0.1
0.08
0.06
0.04
0.02
0
80
160
240
320
400
480
560
640
Time (s)

Figure S5